Measurement of combustion fluctuations in turbulent premixed methane/air burner and high pressure oil burner

Yuji IKEDA
Department of Mechanical Engineering, Kobe University
Rokkodai, Nada, Kobe 657-8501 JAPAN

And

Laurent ZIMMER
National Aerospace Laboratory of Japan
7-44-1, Jindaiji, Higashi-machi, Choufu, Tokyo 182-8522 JAPAN

The local chemiluminescence of excited radicals such as OH*, CH* or C2* can be used to measure the local equivalence ratio. Furthermore, using high repetition rate acquisition system, it is possible to measure the flame passing frequency and to determine the width of the flame front. When using simultaneously three detectors, the velocity can be measured. This technique is applied to a turbulent premixed burner to estimate its accuracy. Typical uncertainties are below 4%. When using Cassegrain optics in a high pressure oil burner, oscillations are measured and their frequency can be determined.

1. INTRODUCTION

In order to control the turbulent combustion [1-3] for reducing pollutant [4-6], increasing combustion efficiency [7] and obtaining stable flame holding [8-11], we have to know more detailed structure at turbulent flame-front. Local flame-front structures have been investigated to determine effects of turbulence - chemistry interaction, vortex interaction with the flame-front, stretch rate, flame curvature, extinction, and equivalence ratio [12-26]. Turbulent flames can be defined by the chemical reaction at the flame-front affected by turbulence, so it is necessary for combustion diagnostics to have a high spatial and temporal resolution.

Laser techniques have greatly been playing a major role to measure flame-front structures and their features under various conditions. Laser-induced fluorescence (LIF) [27-29] becomes a very powerful tool to visualize the OH*/CH*/C_2* reaction zone and its time evolution [30]. LIF techniques [27, 31, 32] can provide useful 2-dimensional information on flame shape and flame front structure, but time-series analysis of the flame front structure could not be demonstrated because the laser repetition rate.

The chemiluminescent emissions from excited OH, CH and C_2 originate from the chemical production of the excited states. Even by LIF, the ground state radical concentration can be measured. Chemiluminescence measurements are needed in reaction modeling to predict excited radical concentrations, but what we can actually measure is not the excited radical concentrations but the intensity of chemiluminescent emissions [33-37].

In order to measure the chemical reaction scale and the flame-front structure with high temporal and spatial resolutions, Cassegrain optics were developed that are capable of measuring local chemiluminescences (OH*, CH*, C_2*) in a small control volume (0.1×0.8 mm) [38, 39]. The size of the measurement volume was sufficiently small as to detect the flame-front location and reaction intensities profiles.

We have applied this local chemiluminescence measurement in a laminar premixed flame [40], a turbulent flame [41-44] and a SI engine [45, 46]. The local measurement system has been evaluated and the measurement results could provide useful information such as, local equivalence ratio, flame thickness, flame passing frequency, detail radical profile within the flame front.

In this study, we developed 3-point local chemiluminescence measurement system in a turbulent premixed flame to measure local equivalence ratio in time series, its flame passing frequency and its moving characteristics.

This chemiluminescence measurement system was applied to understand combustion fluctuation [8, 47, 48] in a practical oil burner at elevated pressure [47][49-53], which is a pilot burner of industrial gas turbine combustor [7].

2. EXPERIMENTAL APPARATUS

2.1. Turbulent premixed flame

The experiments were carried out using a turbulent premixed burner of 20 mm inner diameter, Reynolds number of 8100, mean velocity U of 4.0m/s, RMS velocity u' of 0.32m/s. Methane was used as fuel at an equivalence ratio ϕ of 1.0, where the laminar burning velocity S_L is 0.37 m/s. As $u'/S_L = 0.86$, the wrinkled flame regime is expected and the laminar velocity of the flame predominates.

Cassegrain optics was developed [38, 39] the measurement volume dimensions are shown in Fig. 1. A small measurement volume of ϕ 0.1×0.8 mm was achieved to produce a spatial resolution similar to that of Laser Doppler Velocimetry [54]. The simultaneous measurement system for the local chemiluminescences of OH*, CH* and C_2* is also shown in Fig. 2. Flame emissions from excited species received by Cassegrain optics was focused onto an optical fiber (quartz, core: 200μm diameter), transmitted to band-pass filtered (BPF) spectroscopy unit and photo-multipliers (PMT). The analog output signals of these PMT were amplified, filtered, and digitized by a multi-channel A/D converter at a sampling rate of 200 kHz. The large memory capacity of the system permitted continuous measurements for several seconds. As shown in the figure, four color splitters (interference and dichroic filters) for OH*, CH*and C_2* were implemented for each radical emissions. The specifications for each of the optical filters were determined as follows (center wavelength / half-band width / transmitting efficiency):

OH*	:	306nm / 14nm / 61%
CH*	:	431.4nm / 1.5nm / 40%
C_2*	:	516.5nm / 2nm / 58%

2.2. High pressure oil burner

For elevated pressure conditions, the test nozzle assembly, which had a vertical traverse system, was mounted in a pressure vessel of 230 mm in inner diameter and 1,300 mm in vertical length. It could operate at pressures up to 5.0 MPa. The combustion chamber was designed with purged quartz windows, through which laser diagnostics and chemiluminescence measurements of combusting spray could be made from outside the combustion chamber. Highly pressurized air was supplied to the vessel from a high-pressure air tank, which had a 32-m^3 capacity and held compressed air charged by a compressor. A heat exchanger was installed between the high-pressure air tank and the vessel; this used combustion exhaust gas to heat the air to around 400 °C (673 K). The maximum mass flow rate of the high-pressure air was 7kg/s. Light oil was pressurized by a fuel pump and sprayed into the vessel. The pressure vessel was carefully designed [55-57], and much attention was paid to the size and location of the optical windows used to measure phase Doppler anemometry (PDA) [58-62] and laser simultaneously.

High-pressure air passed through axial swirler vanes surrounding the nozzle, and was then ejected at the swirler exit, which had an inner diameter of 81 mm. At the tip of the nozzle body, which had an outer diameter of 54 mm, a pressure-swirl atomizer (DELAVAN Inc.) was mounted on the central axis of the nozzle. The flow rate of the atomizer was 35 GPH (gallons per hour), and a spray angle of 80° was chosen to create a hollow-cone spray.

3. RESULTS AND DISCUSSION

3.1. Turbulent flame

3.1.1. Local Equivalence Ratio and its time Series

The instantaneous flow vectors were measured by PIV system [30] as shown Fig. 3. In order to understand turbulent characteristics, two measurement points were chosen, as flame cone as illustrated in the figure.

Time-series signals of OH*, CH* and C_2* chemiluminescences at the Cone (r/R=0.4, x/D=2.8) of flame are measured by this system, at 200 kHz sampling rate as shown in Fig. 4. Each intensity of chemiluminescence was normalized by each maximum peak value. These three time traces of chemiluminescence intensity peak and its location synchronized each other very well. The usefulness of Cassegrain optics for understanding local combustion intensity and flame movement is proven in this measurement. Here, each peak intensity of these three radicals, is varying in time and position, this is mainly because the variation of local equivalence ratio.

Here, it is found that the time depending flame front structure can be defined by this measured system in terms of local equivalence ratio and flame passing interval. There are some un-known factors remained, such as effects of flame stretch, curvature, strain rate, temperature, pressure, and so on, which are current research subjects going on.

In our previous study [40], the ratio of the C_2*/CH* and the OH*/CH* versus equivalence ratio for the local flame front of a laminar premixed flame was investigated and found a strong correlation. These results showed that the relationships between these curves and the equivalence ratio were nearly linear when the equivalence ratio was less than

1.4 as shown in Fig. 5. This high degree of correlation indicated that the local equivalence ratio at the flame front can be determined by spatially resolved chemiluminescence measurements. In the same matter, equations for prediction of local equivalence ratio can be derived as presented in Fig. 5.

In the present study, we applied this technique to analyze turbulent premixed flames in order to detect the local equivalence ratio at the flame front in time series. We confirmed that the same correlations between local equivalence ratio and local emission intensity ratio were obtained with the error of 5% in previous studies [40-43].

The local equivalence ratio at a local flame-front was directly measured in turbulent methane/air premixed flames using the correlation formula of OH*/CH* based on laminar flame results. Figure 6 shows the time evolution of instantaneous local equivalence ratio of flame front at the Cone of turbulent premixed flames.

Probability density functions (PDF) of the instantaneous local equivalence ratio are also shown. The mean measured local equivalence ratios were 0.96, 1.04, and 0.98 at the cone for a pre-set equivalence ratio of 1.0. The RMS of the local equivalence ratio was less than 0.2. The detection accuracy of the local equivalence ratio in the present study was 4%.

These time-series measurements of the flame-front structure can also provide the flame passing frequency, as shown in Fig. 7. The average frequency at the flame cone was 0.39 kHz.

3.1.2. Multi-point Local Chemiluminescence signals

To investigate the local flame front movement and its velocity vector, multi-point Cassegrain Optics were used for simultaneous time-resolved measurement of local chemiluminescence emission intensities at three different points in the turbulent premixed flame. The locations of the measurements and a sketch of the local chemiluminescence intensity signals are shown in Fig. 8 [63, 64]. Three similar peaks would be seen if a locally flat flame front passed through each measurement point; and the flame front speed and direction would be defined by the periods τ_1 and τ_2, which are expressed as:

$$\tau_1 = \frac{d_1 \cdot \sin\left(\frac{\pi}{2} - \theta_f\right)}{V_f} \qquad (1)$$

and

$$\tau_2 = \frac{d_2 \cdot \sin\left[\alpha - \left(\frac{\pi}{2} - \theta_f\right)\right]}{V_f} \qquad (2)$$

where V_f and θ_f are defined as the local flame velocity and flame displacement angle for a horizontal surface; d_1 and d_2 are the distance between measurement points a and b, and b and c, respectively; and α is the interior angle of the equilateral triangle formed by the three measurement points.

From Eqs. (1) and (2), for $\tau_2 \neq 0$, V_f and θ_f are:

$$\theta_f = \cot\left(\frac{\tau_1 + 2\tau_2}{\sqrt{3}}\right) \qquad (3)$$

and

$$V_f = \frac{d \cdot \sin\left(\frac{\pi}{2} - \theta_f\right)}{\tau_1} \qquad (4)$$

and for $\tau_2 = 0$, V_f and θ_f are:

$$\theta_f = \frac{\pi}{2} \qquad (5)$$

and

$$V_f = \frac{d \cdot \sin\frac{\pi}{3}}{\tau_2} \qquad (6)$$

where V_f is defined as a positive.

3.1.3. Local flame front movement

The typical local chemiluminescence emissions measured by multi-point Cassegrain Optics at point (r/R=0.4, x/D=2.8) in a turbulent premixed flame in the wrinkled laminar flame region. Irregular peaks, which represent the passage of the flame front, correspond with each other well, although there is a time delay between the peaks. V_f and θ_f for the local flame front were obtained from a series of chemiluminescence signals using the above-mentioned scheme.

In this study, only sharp emission intensity peaks exceeding a certain level were used to determine V_f and θ_f in order to reduce errors in calculating these values. If the flame front passed through the control volume along the Cassegrain optical axis, the calculated velocity of the flame would be extremely high because the flame front would arrive at all the measurement points at nearly the same time. In this case, however, the peak profile of the emission signals would not be sharp and the peak intensity would be less than when the flame front crossed the control volume perpendicular to the optical axis. By using only the sharp peaks in the data, we should avoid this error. The sensitivity of the Cassegrain Optics system to the flame front configuration requires further evaluation.

The local flame front measurement was investigated using this multipoint system. The local flame speed and its propagating angle as well as its thickness were measured in flame cone (Fig. 9).

The flame propagating speed at flame tip was about 3.4 m/s, where the flame propagating flow velocity was 4.0 m/s. The flame propagating angle was about 28 degree, which means the flame is propagating in vertical direction with fluctuating.

On the other hand, at flame cone, the flame propagating speed is about 0.7 m/s, which means that the flame front is stable at flame cone. The flame propagating angle was about 53 degree. This 53 was due to the flame front inclination. This turbulent flame is not so strong turbulence, like winkled turbulent flame. The flame thickness at flame cone was about 5.7 m/s, which is large in comparison with the laminar flame front thickness. This value can be reduced with optical filter in smoothing process of each sample.

In this study, it was found that emission intensity ratio for OH*/CH*, C_2*/CH*, and C_2*/OH*can be a good marker of local equivalence ratio at the turbulent premixed flame-front. The accuracy of detection of local equivalence ratio at the present study was about 7 %. In the next study, un-known factors such as effects of strain rate and temperature will be investigated.

3.2 High pressure oil burner

3.2.1. Experimental facility

Experiments in the combustion field were conducted under a fixed air temperature of 400°C (673K) and an airflow rate of 0.172 m^3/s. The ambient air pressure was varied from 0.25 to 2.5 MPa. In this study, the fuel-to-air ratio (F/A) was fixed at 1.5(wt.%). Diesel fuel was injected from the nozzle and the fuel flow rate was varied from 38.3 to 218.9 kg/h depending on the atmospheric pressure.

Figure 10 shows direct-observation-averaged and instantaneous images of the flame formed in the pressure vessel at 0.25, 1.0, and 2.0MPa. As seen in the figures, the flame had a triangular cone shape, which was essentially the same at each pressure. The averaged and instantaneous flame-spreading angle can be measured from the images. Although the fuel and air were supplied at constant conditions, the complicated wrinkled structure of the flame seen in the instantaneous images indicates that it was a turbulent spray flame. The flame intensity distribution and length fluctuated strongly in time and space. Looking at the averaged images, the spatial structure of the flame and the characteristics at each pressure condition can be observed briefly.

In the images at 0.25MPa, a bright region was observed around the nozzle exit and a similar region was seen upstream from the nozzle, due to the reversing flow around the nozzle. High intensity regions were also formed at the flame edge. Reaction radicals and scattered light from soot particles were the source of these high intensity regions. Inside the hollow cone structure, where we found a reverse flow region during cold flow measurements, the emission intensity was lower than at the edge of the surrounding flame. The instantaneous pictures were taken with a 100μs exposure. The features of the high-intensity regions could not be seen in the averaged pictures. The flame-spreading angle was almost the same in both the instantaneous and averaged images.

Now, we will discuss changes in the flame spreading angle and the location of the flame front region with changes of surrounding pressure. The spray droplets from the nozzle traveled at an angle, evaporated, and combusted, but it is difficult to see these droplet behaviors by viewing these images alone. The detailed droplet dynamics will be discussed later.

At 1.0MPa, a wrinkled flame structure was apparent in the instantaneous image. Furthermore, two high-intensity regions were also observed, and were even seen in the averaged image. The flame-spreading angle was slightly narrower and the flame extended further downstream than in the images at 0.25MPa. At 2.0MPa, the flame-spreading angle was very narrow in comparison with 0.25 and 1.0MPa. The flame was also longer. This was essentially due to the experimental conditions. The higher-pressure condition had much more fuel and air, but a constant equivalence ratio. When the pressure increased, the flame appeared to stretch vertically. Moreover, the other important consequence of increasing the surrounding pressure was that the flame-spreading angle from the nozzle narrowed. One possible reason for this narrowing is that the hollow cone angle of the fuel droplets changes due to the effect of the surrounding airflow structure. On the 1.0MPa images, the flame expanded horizontally in the middle stream due to volumetric expansion and centrifugal force caused by the swirling airflow. At 2.0MPa, the flame-spreading angle was narrower and the flame stretched vertically.

The flame-spreading angles in the averaged images do not differ from those in the instantaneous images. In all conditions, two higher-intensity regions are seen: one close to the nozzle and one near the flame front. These are formed by emission of soot or other radicals, and will be examined in the CH* images of flames. The figure also shows the CH* chemiluminescence [40] intensity distribution. The relationship between pressure and flame shape (flame-spreading angle and vertical length) is easily seen. The trend seen in the direct observation images with increasing pressure is also seen, i.e., the flame-spreading angle narrows and the flame extends vertically. Although the CH* filtered image showed a different angle at 2.0MPa, the increased atmospheric pressure still narrowed the flame angle. On the CH* images, two high-intensity regions were clearly seen. At the edge of the hollow cone, CH* radicals were formed and the intensity increased with atmospheric pressure.

Figure 11 shows the change in the spreading angles and lengths of the flame as a function of ambient pressure from 0.25 to 2.0MPa. These values were measured directly from the images. As the ambient pressure increases, the flame lengthens, while the spreading angle narrows. The CH*-spreading angle was wider than the flame. We found that the ambient pressure affected the flame-spreading angle. One possible reason for the change in flame angle is the increased pressure difference between inside and outside the hollow spray cone with increasing ambient pressure. Next, we will quantify the relationship between ambient pressure and spray angle.

3.2.2. Droplet behavior measurement by PDA

The previous section described the change in spray flame-spreading angle with ambient pressure. To grasp the characteristics of flame structure and droplet behavior in more detail, PDA was applied to flow fields at 0.25, 0.5, and 0.75MPa. The vector maps for each pressure condition acquired by PDA are shown in Fig. 12. At x=15mm and x=35mm there are some vectors with a strong radial component. This is another possible explanation for the horizontal expansion of the flame that we found in the image analysis.

3.2.3. Chemiluminescence measurement in an oil burner

At the flame front, the flame fronts are fluctuating. The combustion oscillation and its instability come from local heat release rate and its fluctuation in space and time.

As we observed in the premixed turbulent flame, the fluctuation can be measured with Cassegrain technique. The measurement system of local chemiluminescence was the same as those used in the turbulent burner. The time series chemiluminescence data is shown in Fig. 13. Figure 13 shows two measurement results at 0.25 and 2.0MPa. The equivalence ratio of the combustion was set up at ϕ=1.0 but air flow rate and fuel rate was almost ten times higher at 2.0MPa. The flame picture shows the enlarged flame. The chemiluminescence signals in time were shown in this figure, in which OH*and CH* were indicating same tendency and fluctuation. The peak location seems to be the same; the local equivalence ratio can be measured if the calibration curve is measured in advance. But this correlation, the intensity ratio of OH*/CH* being a function of local equivalence ratio, cannot obtained so far for oil fuel.

The local heat release being a good maker for combustion oscillation and instability, the local chemiluminescence measurement results can be analyzed in frequency domain. The FFT data was shown in Fig. 14. A hundred thousand sampling was done at each measurement point. There is no remarkable peak up to 1.0MPa, while the peak comes from 1.5MPa and 2.0MPa. The peak can be the same order both in OH* and CH*signals. The measurement point was illustrated in Fig. 13, where is at the flame front.

It is not well known that combustion oscillation was yielded at flame front or not, but it is clear that the flame front movement generate local heat release at different location.

The Cassegrain measurement techniques were demonstrate to see the fluctuation at flame front. We shall see the correlation to pressure fraction and flow fluctuation and those phase delay.

4. CONCLUSIONS

Time-series measurements of the local chemiluminescence intensities of OH*, CH* and C_2* were obtained for a premixed turbulent flame to elucidate the flame front structure and its time evolution. The findings were as follows:

- Local measurements of flame spectra and its time evolution to elucidate local flame structure was demonstrated using Cassegrain optics developed for a turbulent premixed flame.

- The local equivalence ratio was measured from the emission intensity ratio of OH*/CH*, CH*/C_2* and C_2*/OH* at flame tip and cone in the turbulent premixed flame-front. The estimated value is very close to preset value of 1.0. The accuracy was 4%.

- The flame passing frequency was obtained by time series chemiluminescence measurements. There was a 2 kHz peak at the flame tip, but no peak at the flame cone.

- The local flame front velocity and its angle were measured by these point measurements.

- Direct observation images showed flame shape and length together with the spray-spreading angle. With increasing ambient pressure, the flame lengthened due to increased fuel, and the spray angle narrowed.

- CH* distribution images showed the same changes; with increasing pressure the spray angle narrowed.

- CH* distribution images showed that the spreading angle was bigger than the flame itself and the area of distribution was slightly bigger than that of the flame.

- PDA was used to quantify the spray angle at each pressure; the results also showed that as the ambient air

- Chemiluminescence measurement in an oil burner can detect flame front movement at flame edge. The time series data of OH* and CH* can show some order 20Hz were produced at elevated pressure of 1.5 and 2.0MPa, although these peaks cannot be measured below 1.0MPa.

REFERENCES

[1] Johnson, C. E., Neumeier, Y., Lieuwen, T. and Zinn, B. T., Proc. Comb. Inst. 28: 757(2000)
[2] Neumeier, Y. and Zinn, B. T., AIAA-96-0758 (1996)
[3] Van Dyken, R., Yu, K., Gutmark, E., Tuncer, I., Platzer, M., McLachlan, B. and Bell, J., AIAA-96-0248 (1996)
[4] Lefebvre, A. H., Gas Turbine Combustion (2nd ed), Taylor & Francis, Philadelphia, 1999
[5] Grosshandler, W., Hamins, A., McGrattan, K. and Rao Charagundla, S. and Presser, C., Proc. Comb. Inst. 28: 2957 (2000)
[6] Demayo, T. N., Miyasato, M. M. and Samuelsen, G. S., Proc. Comb. Inst. 27: 1283 (1998)
[7] Kuo, K. K., Principles of Combustion, John Wiley and Sons, Inc., NY, 1986
[8] Hayashi, S., Yamada, H., Shimodaira, K. and Machida, T., Proc. Comb. Inst. 27: 1833 (1998)
[9] Lieuwen, T. and Zinn, B. T., Proc. Comb. Inst. 27: 1809 (1998)
[10] Matta, L. M., Wuersig, A., Choung, D., Jagoda, J. I. and Zinn, B. T, AIAA-96-0642 (1996)
[11] Paschereit, C. O., Gutmark, E., Weisenstein, W., Proc. Comb. Inst. 27: 1887 (2000)
[12] Damköhler, G. and Jahrb, Z., *Elektrochem*, 46:601-627 (1940)
[13] Poinsot, T., Veynante, D., and Candel S., *Proc. Combust. Inst.* 21, (1990), 613-619
[14] Furukawa, J., *Proc. Combust. Inst.* 25, (1994), 1233-1239
[15] Summerfield, M., Riter, S.H., Kebely V. and Mascolo R.W., Jet Propulsion 25:377 (1955)
[16] Karlovitz, B., Dennision, D.W. and Wells, F.E., J. Chem. Phys. 19:541 (1951)
[17] Williams, F.A., Combustion Theory (2nd ed) Addison-Wisley, Redwood City, 1985
[18] Furukawa, J., Toshisuke, H. and Williams, F.A., Combust. Flame 113:487 (1998)
[19] Bedat, B. and Cheng, R.K., Combust. Flame 100:485 (1995)
[20] Poinsot, T., Veynante, D. and Candel, S., J. Fluid Mech. 228:561 (1990)
[21] Ashurst, W.T. and Barr, P.K., Combust. Sci. Technol. 34: 227 (1983)
[22] Yoshida, A., Kakinuma, H. and Kotani, Y., Proc. Combust. Inst. 26:397 (1996)
[23] Law, C.K., Proc. Combust Inst. 22:1381 (1988)
[24] Peters, N., Proc. Combust Inst. 21:1231 (1986)
[25] Ishizuka, S., Proc. Combust Inst. 20:287 (1984)
[26] Platt, J.A., and Tien, J.S., Chemical and Physical Process in Combustion, Fall Technical Meeting, Eastern Section of the Combustion Institute, 1990, p. 31

[27] Buschman, A., Dinkelacker, F., Schäfer,M. and Wolfrum, J., *Proc. Combust. Inst.* 26, (1996),437-445
[28] Han, D., Mungal, M.G., Proc. Combust. Inst. 28:261 (2000)
[29] Barlow, R.S., Fiechtner, G.J. and Chen, J.-Y., Proc. Combust Inst. 26:2199 (1996)
[30] Nguyen, Quang-Viet. and Paul, P.H., *Proc. Combust. Inst.* 26, (1996), 357-364
[31] Hanson, R.K., Proc. Combust Inst. 22:1877 (1988)
[32] Muniz, L. and Mungal, M.G., Combust. Flame 1126:1402 (2001)
[33] Gaydon, A.G., "*The Spectroscopy of Flames*," Chapmann and Hall, 1974
[34] Walsh, K. T., Long, M. B. Tanoff, M. A. and Smooke M. D., *Proc. Combust. Inst.* 27, (1998), 615-623
[35] Walsh, K.T., Fielding, J., Smooke, M.D. and Long, M.B., Combust. Inst. 28:1973 (2000)
[36] Najm, H. N., Paul, P. H., Mueller, C. J., and Wyckoff, P. S., *Combust. Flame* 113:312-332(1998)
[37] Samaniego, J. M., and Mantel, T., *Combust. Flame* 118:537-556(1999)
[38] Akamatsu, F., Wakabayashi, T., Tsushima, S., Katsuki, M., Mizutani, Y., Ikeda, Y., Kawahara, N., and Nakajima, T., *Meas. Sci. Technol.* 10, No.12 (1999), 1240-1246
[39] Ikeda, Y., Ichi, S., Nakai, H., and Nakajima, T., COMODIA98, (1998), pp.411-416
[40] Kojima, J., Ikeda, Y. and Nakajima, T., *Proc. Combust Inst.* 28, (2000). In press
[41] Ikeda, Y., Kojima, J. and Nakajima, T., *Proc. Combust Inst.* 28, (2000). In press
[42] Kojima, J., Ikeda, Y., and Nakajima, T., 35th AIAA/ASME/SAE/ASEE Joint Propulsion Conference and Exhibit, AIAA paper 99-2784
[43] Kojima, J., Ikeda, Y., and Nakajima, T., 36th AIAA/ASME/SAE/ASEE Joint Propulsion Conference and Exhibit, AIAA paper 2000-3394
[44] Ikeda, Y., Kojima, J., and Nakajima, T., 36th AIAA/ASME/SAE/ASEE Joint Propulsion Conference and Exhibit, AIAA paper 2000-3395
[45] Ikeda, Y., Kaneko, M., and Nakajima, T., *SAE Transactions* Paper, (1999), No.1999-01-3680
[46] Ikeda, Y., Nishihara, H. and Nakajima, T., *COMODIA2001*, (2001), 637-
[47] Murugappan, S., Gutmark, E. J., Acharya, S. and Krstic, M., Proc. Comb. Inst. 28: 731(2000)
[48] Kan, T., Matta, L. M., Jagoda, J. I. and Zinn, B. T., Proc. Comb. Inst. 28: 2709 (2000)
[49] Wolff-Gassmann, D., Hohmann, S. and Zarzalis, N., Trans. ASME, 123: 810-816 (2001)
[50] Leong, M. Y., Smugeresky, C. S., McDonnell, V. G. and Samuelsen, G. S., Trans. ASME, 123: 574-579 (2001)
[51] Zhu, G. S. and Reitz, R. D., Trans. ASME, 123: 412-418 (2001)
[52] Carl, M., Behrendt, T., Fleing, C., Frodermann, M., Heinze, J., Hassa, C., Meier, U., Wolff-Gassmann, D., Hohmann, S. and Zarzalis, N., Trans. ASME, 123: 810-816 (2001)
[53] Choudhuri, A. R. and Gollahalli, S. R., J. Prop. Power, 17: 190-196 (2001)
[54] Liu, Y. and Lenze, B., *Proc. Combust. Inst.* 22, (1988), 747-754
[55] Taylor, A. M. K. P., Instrumentation for Flows with Combustion, Academic Press, London, 1993
[56] Kawahara, N., Hirohata, T., Ikeda, Y. and Nakajima, T., 8th Int. Symp. on Appl. Of Laser Tech. to Fluid Mech., 1: 10.5.1-10.5.8 (1996)
[57] Ikeda, Y. Hirohata, T. and Nakajima, T, Application of Laser Anemometry to Fluid Mechanics, Springer-Verlag, 1997, p.165
[58] Jasuja, A. K. and Lefebvre, A. H., Proc. Comb. Inst. 25: 345 (1994)
[59] Zheng, Q. P., Jasuja, A. K. and Lefebvre, A. H., Proc. Comb. Inst. 26: 2757 (1996)
[60] Lefebvre, A. H., Atomization and Sprays, Hemisphere Publishing Corporation, NY, 1989
[61] Ateshkadi, A., McDonnell, V. G. and Samuelsen, G. S., Proc. Comb. Inst. 27: 1985(1998)
[62] Ateshkadi, A., McDonnell, V. G. and Samuelsen, G. S., Proc. Comb. Inst. 28: 1281(2000)
[63] Suzuki, T. and Hirano, T., *Proc. Combust. Inst.* 20, (1984), 437-444
[64] Furukawa, J., Hirano, T. and Williams, F.A., Combust. Flame 113:487 (1998)

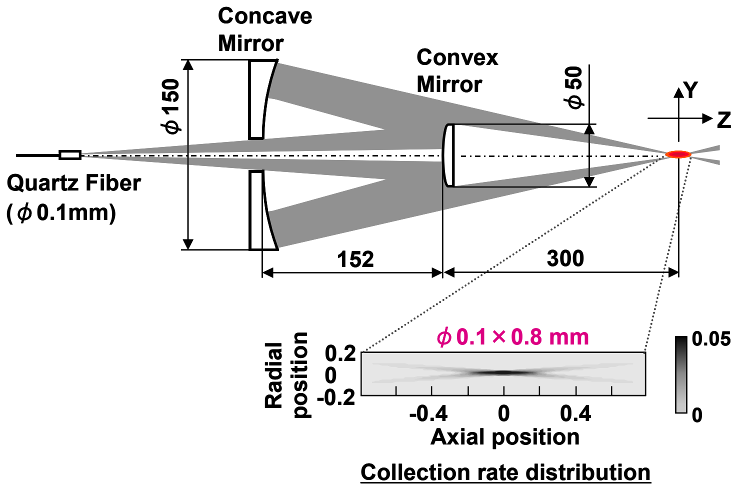

Fig.1 Cassegrain Optics

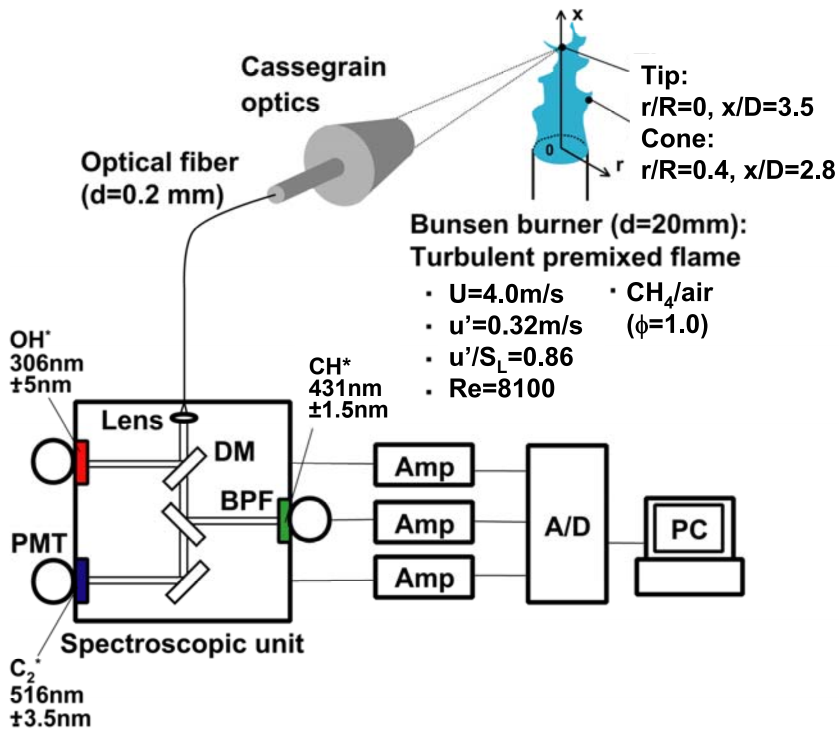

Fig. 2 Experimental apparatus

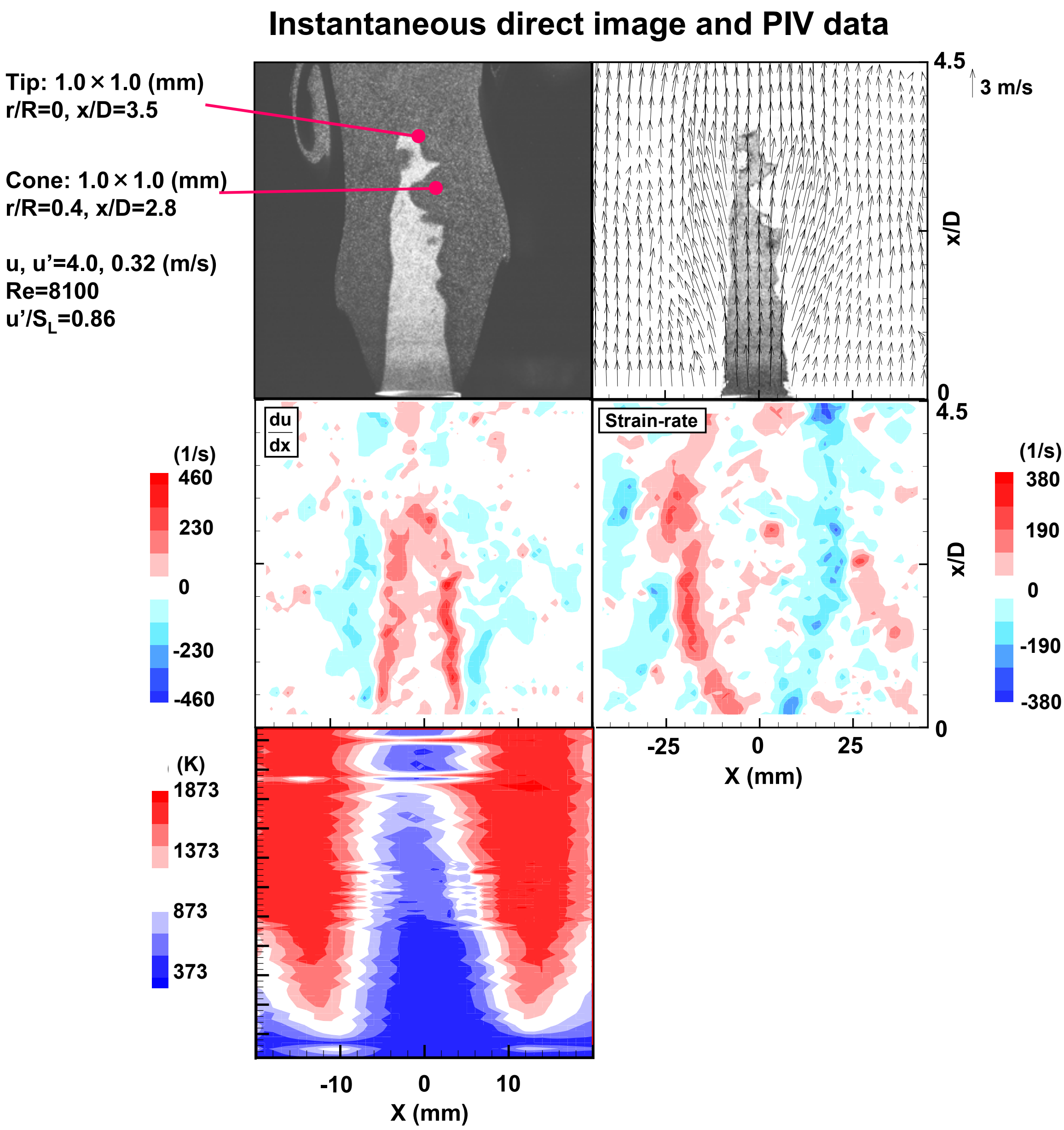

Fig. 3 Instantaneous direct image, PIV data and temperature measurement

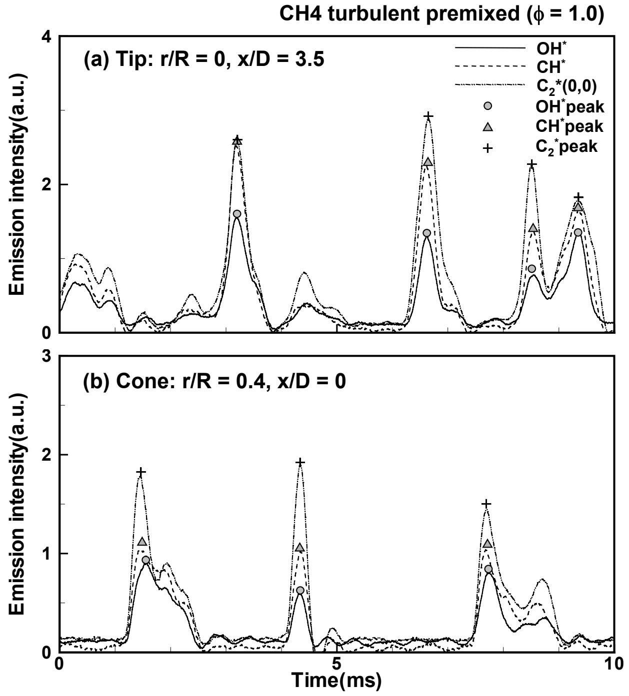

Fig. 4 Peak emission intensities at the flame fronts of turbulent premixed flame

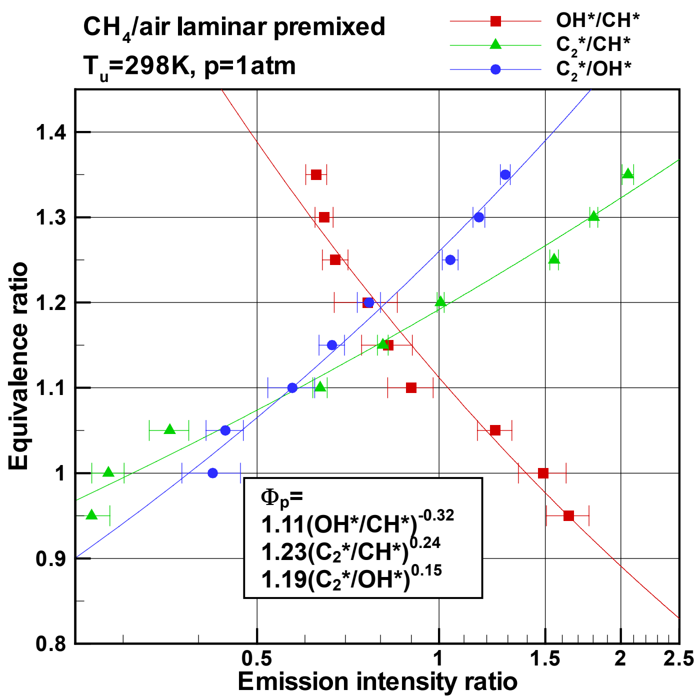

Fig. 5 Correlation of chemiluminescence intensity ratios to equivalence ratio

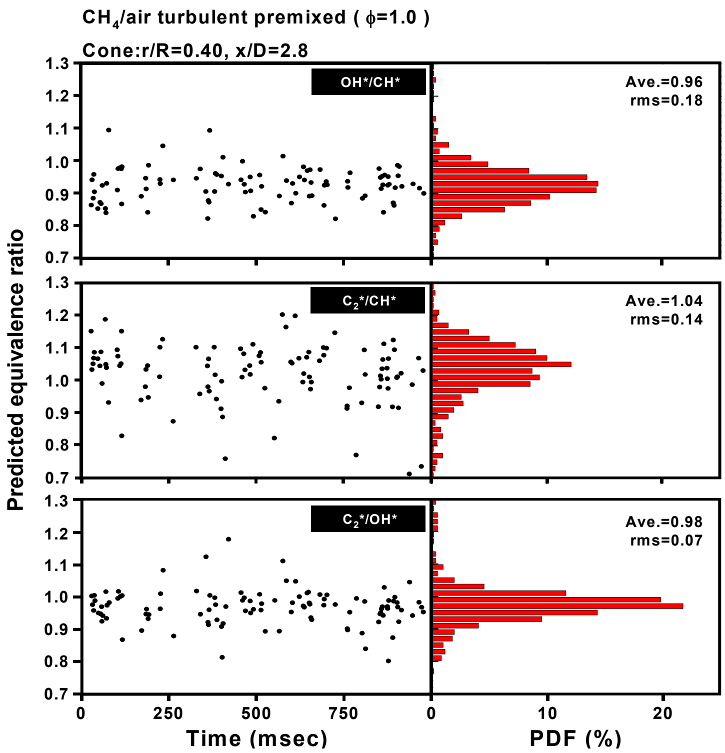

Fig. 6 Time evolution of measured equivalence ratio at local flame fronts

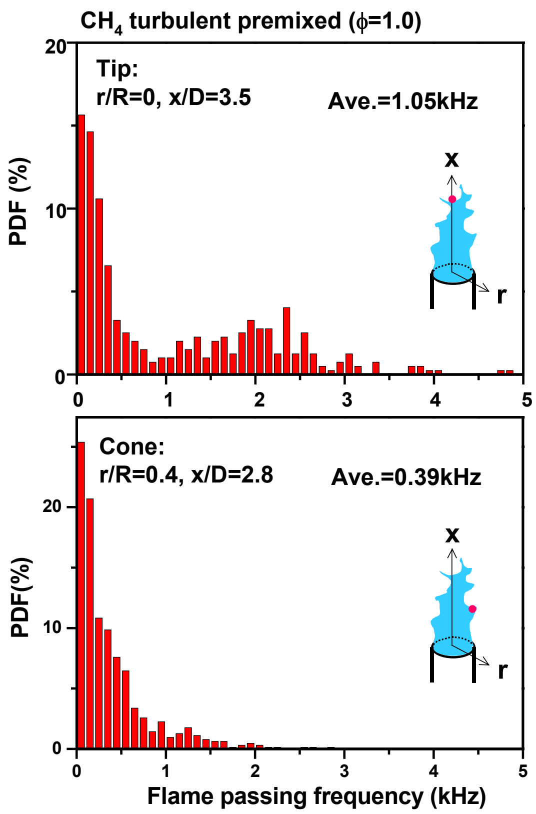

Fig. 7 Flame passing frequency (CH* front)

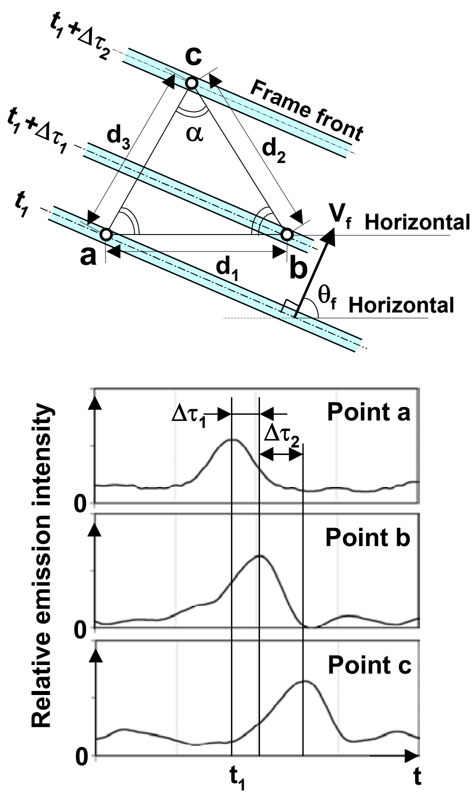

Fig. 8 Three point measurement of local CH* in turbulent premixed flame

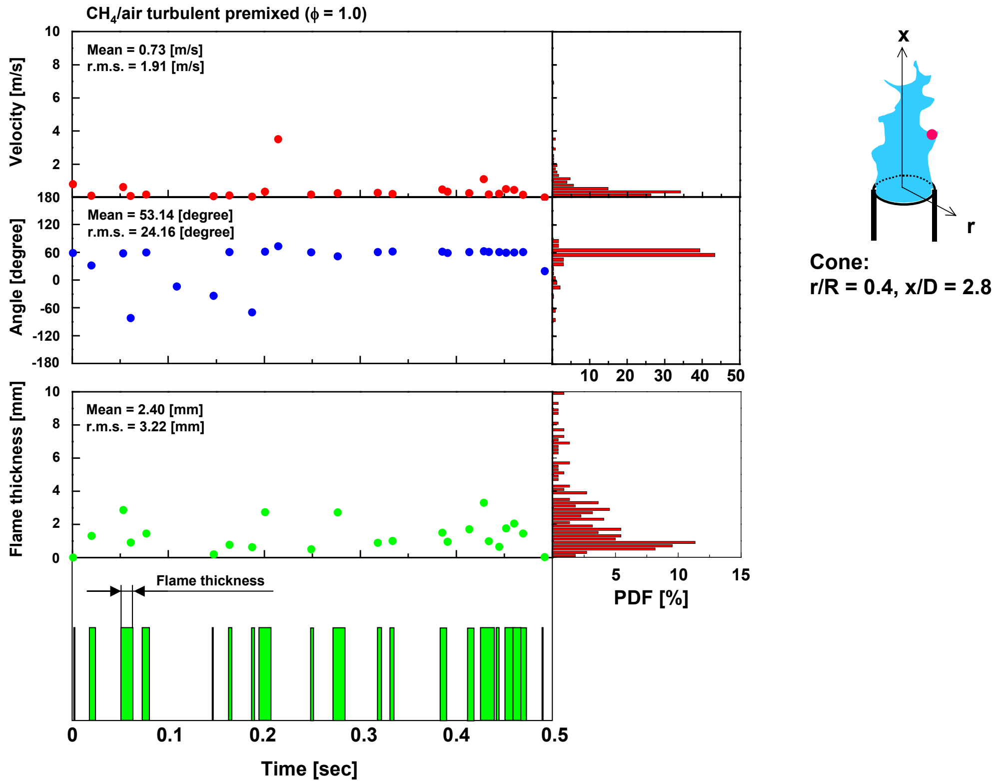

Fig. 1 Time series measurements of flame velocity, flame propagating angle and its thickness at flame cone

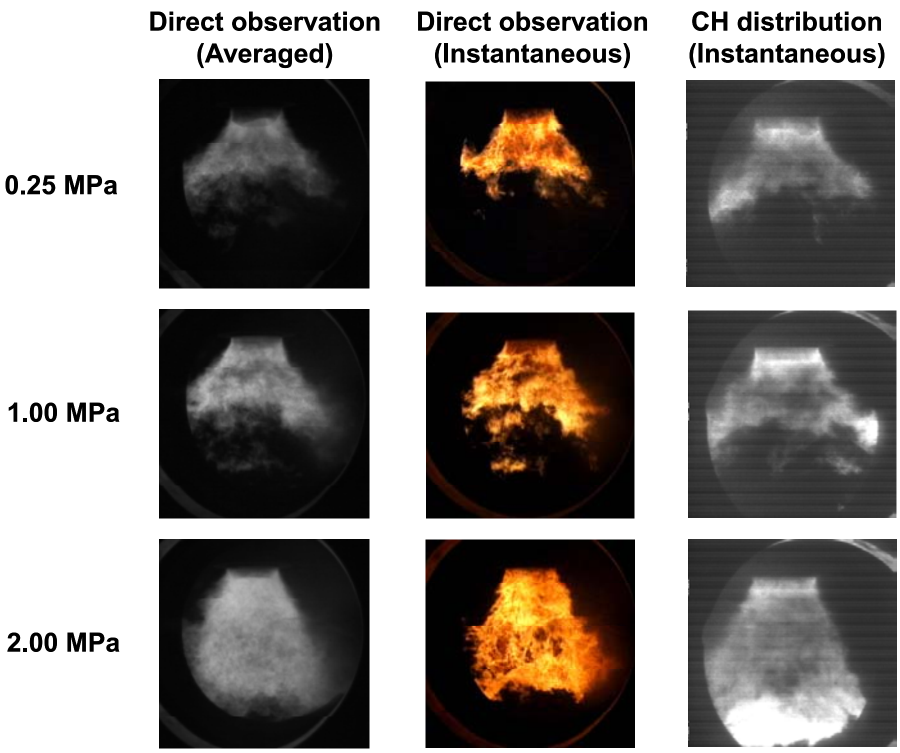

Fig. 10 Flame direct observation and CH* distribution

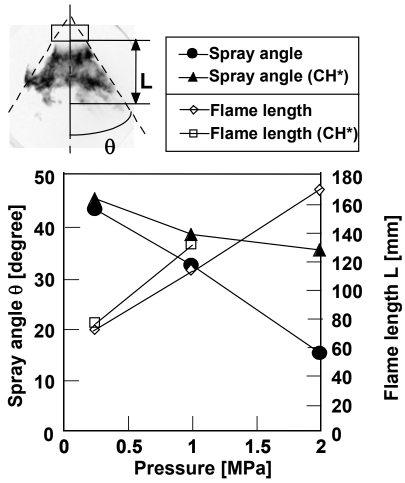

Fig. 11 Flame spreading angle and flame length

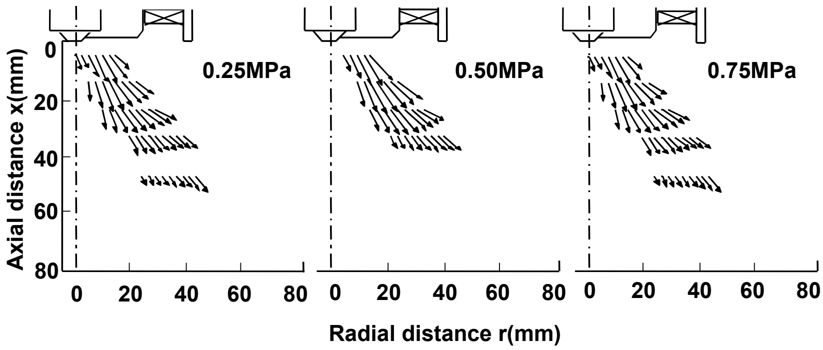

Fig. 12 Vector maps for each pressure condition

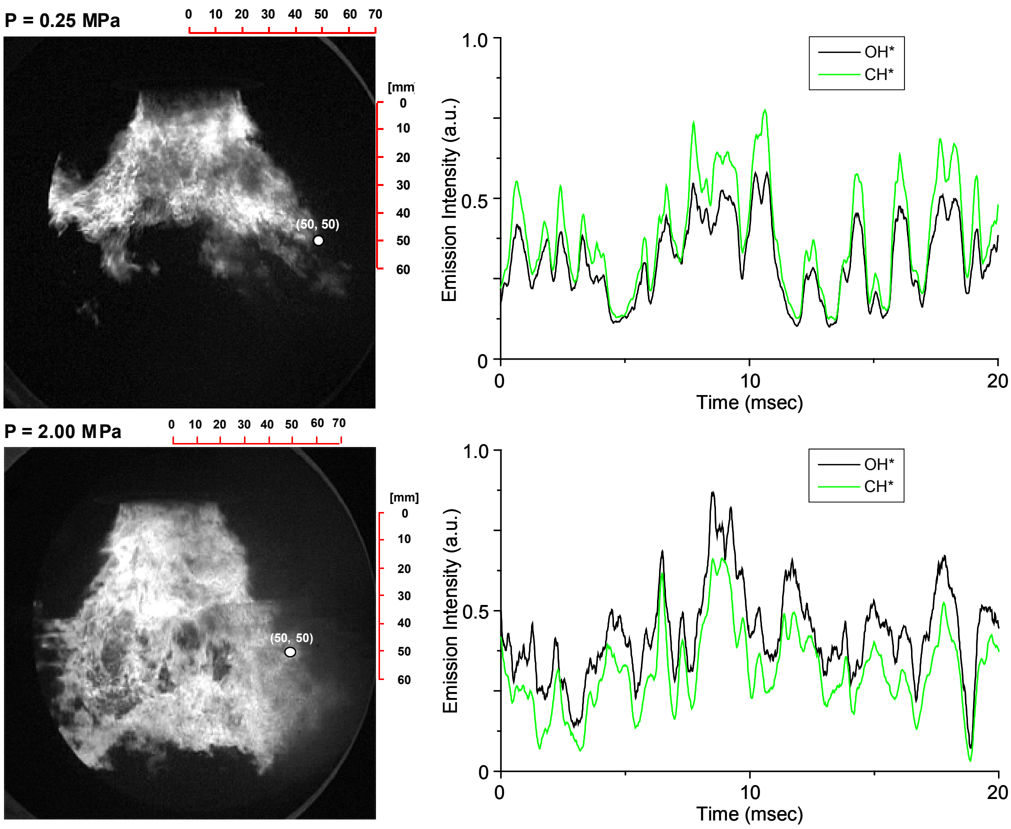

Fig. 13 Time series chemiluminescence of OH* and CH*

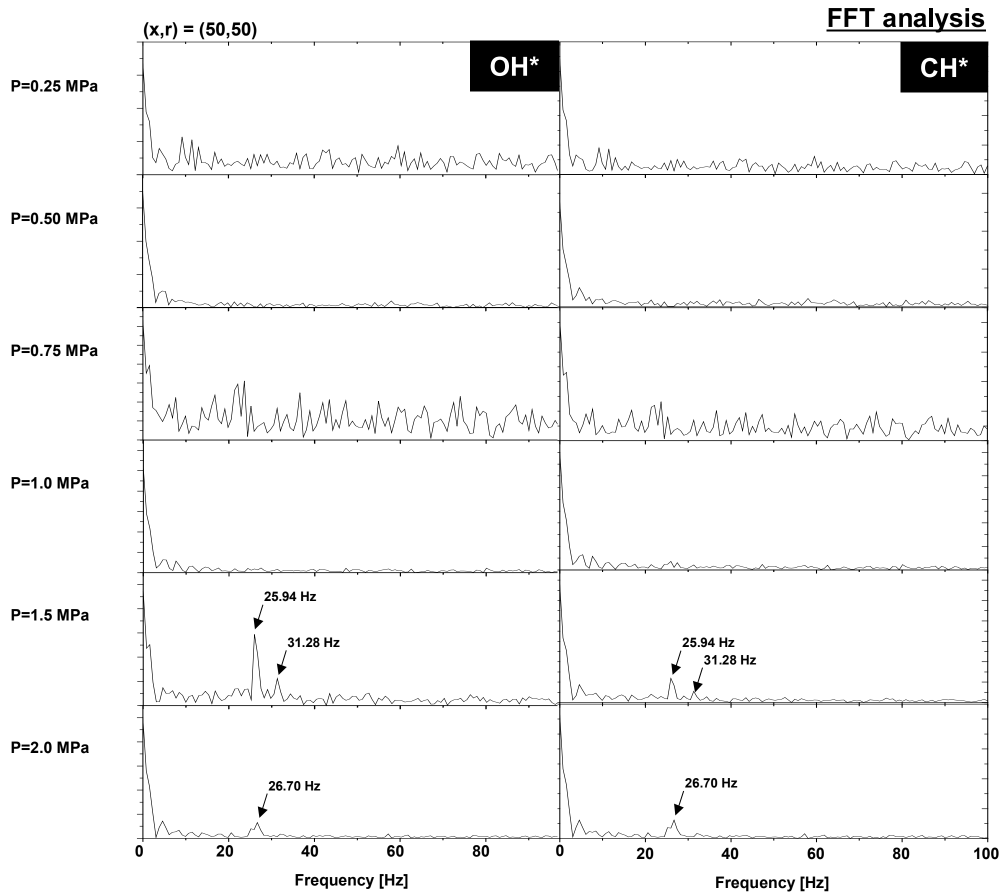

Fig. 14　Frequency analysis of local chemiluminescence of OH* and CH* at flame front